Food Research International xxx (xxxx) xxx–xxx

Contents lists available at ScienceDirect

Food Research International

journal homepage: www.elsevier.com/locate/foodres

Formulation and characterization of O/W nanoemulsions encapsulating high concentration of astaxanthin

Nauman Khalid[a,b], Gaofeng Shu[c], Brenden J. Holland[a], Isao Kobayashi[d], Mitsutoshi Nakajima[c,d], Colin J. Barrow[a,*]

[a] Centre for Chemistry and Biotechnology, Deakin University, Waurn Ponds, Victoria 3217, Australia
[b] School of Food and Agricultural Sciences, University of Management and Technology, Lahore 54000, Pakistan
[c] Graduate School of Life and Environmental Sciences, University of Tsukuba, 1-1-1 Tennoudai, Tsukuba, Ibaraki 305-8572, Japan
[d] Food Research Institute, NARO, 2-1-12 Kannondai, Tsukuba, Ibaraki 305-8642, Japan

ARTICLE INFO

Keywords:
Astaxanthin
Nanoemulsions
Freeze-thaw treatment
Bioaccessibility
Temperature
Storage stability
Encapsulation efficiency

ABSTRACT

This study evaluates the effect of modified lecithin (ML) and sodium caseinate (SC) on the formulation, stability and bioaccessibility of astaxanthin (AXT) loaded oil-in-water (O/W) nanoemulsions. These nanoemulsions were formulated using high-pressure homogenization in four passes at 100 MPa. The volume mean diameter ($d_{4,3}$) of nanoemulsions produced by ML and SC were 163 ± 5 and 144 ± 12 nm, respectively. The physiochemical stability of nanoemulsions was recorded at 25 °C. The nanoemulsions prepared by ML were stable for 30 minutes against a wide range of pH and heating temperatures (60–120 °C). However, ML-stabilized nanoemulsions showed droplet growth when treated at high NaCl concentrations. In comparison, droplet growth was observed in SC-stabilized nanoemulsions at pH 4 and at high temperature treatment. However, SC-stabilized nanoemulsions were stable at high NaCl concentration (500 mM). The SC-stabilized nanoemulsions showed good physical and chemical stability (> 70%) after 30 days of storage. The bioaccessibility of AXT in nanoemulsions was significantly higher in ML (33%) than in SC-stabilized nanoemulsions (6%), indicating a strong influence of emulsifier on bioaccessibility. These findings provide valuable information in designing nutritional products such as aqueous based AXT fortified beverages.

1. Introduction

The consumption of marine based food is generally considered healthy and this food provides important nutritional bioactive ingredients, such as long-chain polyunsaturated fatty acids (LCPUFA) and astaxanthin (AXT), that are difficult to obtain from terrestrial food (Shahidi & Ambigaipalan, 2015). Due to the lack of availability of fresh seafood in many locations, and the low overall consumption of some essential ingredients such as LCPUFA, these ingredients are stabilized and added to other food, producing functional foods, or consumed as nutritional supplements. Among the marine based ingredients, omega-3 LCPUFA, glucosamine, squalene, vitamin A, vitamin E and carotenoids such as AXT are of particular commercial interest (Shahidi & Ambigaipalan, 2015). AXT has a range of health benefits that are at least partially due to its potent antioxidant activity (Chen & Kotani, 2016; Dose et al., 2016).

The list of functional attributes of AXT are long and include reduction in inflammatory activity (Chen & Kotani, 2016), improved heart functionality (Zhang et al., 2017), prevention of cataracts (Ishikawa et al., 2015), reduced oxidative stress (Xu, Zhu, Yin, & Ding, 2015) and reduction in cancer cell proliferation (Chen et al., 2017). Besides nutraceutical applications, AXT is used in aquaculture as a natural colorant, particularly for salmanoids (Lerfall, Bendiksen, Olsen, Morrice, & Østerlie, 2016). Despite having substantial health benefits, AXT is a highly unstable compound (Foss et al., 2005) that is prone to degradation due to oxidation, heat stress, pH changes and light (Liu, McClements, Cao, & Xiao, 2016; Taksima, Limpawattana, & Klaypradit, 2015).

Color fading is indicative of AXT degradation and directly correlated with loss of functional attributes (Liu et al., 2016). Moreover, AXT has low bioavailability and low water solubility, which limits its use in functional beverages and foods. There are numerous techniques that can increase the bioavailability of AXT, such as structural modification, emulsification, or microencapsulation. Numerous studies showed improved functionality of AXT in nanodispersions, liposomes and nanoemulsions (Anarjan & Tan, 2013b; Kittikaiwan, Powthongsook, Pavasant, & Shotipruk, 2007; Liu et al., 2016; Ribeiro, Rico, Badolato, & Schubert, 2005; Tachaprutinun,

* Corresponding author at: Centre for Chemistry and Biotechnology, Deakin University, Geelong, Victoria 3217, Australia.
E-mail address: cbarrow@deakin.edu.au (C.J. Barrow).

http://dx.doi.org/10.1016/j.foodres.2017.06.019
Received 25 April 2017; Received in revised form 4 June 2017; Accepted 5 June 2017

Udomsup, Luadthong, & Wanichwecharungruang, 2009). These systems improve the functionality but are highly dependent on system composition, emulsifier selection and end usage (Ozturk & McClements, 2016; Raikos & Ranawana, 2017).

In this study, we attempt to encapsulate high concentrations of AXT extract in O/W nanoemulsions. The nanoemulsions are a colloidal-dispersion system containing small lipid droplets around 20–200 nm dispersed in a continuous aqueous phase (McClements & Rao, 2011; Salvia-Trujillo, Soliva-Fortuny, Rojas-Graü, Martín-Belloso, & McClements, 2017). Due to the small size of the droplets, the nanoemulsions have optical clarity with good stability and oral bioavailability (Gutiérrez et al., 2008; Mason, Wilking, Meleson, Chang, & Graves, 2006; McClements, 2012). Emulsified food products need to be stable against harsh conditions during processing, storage and transportation. The stability of emulsified foods can be increased by optimizing the formulation conditions, like the content and the nature of the emulsifier together with appropriate continuous phase composition (Ozturk & McClements, 2016).

In the current study, two food-grade emulsifiers, namely modified lecithin (ML) and sodium caseinate (SC), were used for evaluating physicochemical stability of AXT loaded O/W nanoemulsions. ML is a zwitter-ion emulsifier with low molecular weight that stabilizes the emulsion system using electrostatic repulsion. The ML used in this study was derived from the hydrolysis of soy lecithin and composed of a range of phospholipids (Shu et al., 2016). SC is a large molecular weight emulsifier derived from bovine milk and stabilized the emulsion system by electrostatic repulsion. In addition, the long tail of disordered casein molecules adsorbed around the oil droplet provides a steric stabilization effect (Surh, Decker, & McClements, 2006).

There are studies that show successful encapsulation of AXT in nanodispersions and nanoemulsions (Affandi, Julianto, & Majeed, 2011; Anarjan, Jafarizadeh Malmiri, Ling, & Tan, 2014; Anarjan & Tan, 2013a). Studies with nanodispersions have used toxic organic solvents like chloroform and dichloromethane to encapsulate AXT, while studies with nanoemulsions use different protein based emulsifiers, but required high purity AXT (> 90% purity) (Anarjan, Mirhosseini, Baharin, & Tan, 2010; Kim, Hyun, Yun, Lee, & Byun, 2012). Most commercial AXT extracts useful for nutritional applications contain only 10 to 20% (w/w) AXT, and are difficult to emulsify due to the presence of various stabilizing ingredients and tocopherols. The objective of this work was to provide a better understanding of the role of emulsifiers in stabilizing O/W nanoemulsions encapsulated high concentration of AXT extract. The *in vitro* digestion behavior and bioaccessibility of AXT loaded nanoemulsions were also investigated in this study.

2. Material and methods

2.1. Materials

Zanthin® (Astaxanthin purity 10%) was procured from Valensa International, FL, USA. Astaxanthin (> 97%) used as reference standard was purchased from Sigma-Aldrich, St. Louis, MO, USA. Pancreatin from porcine pancreas (P7545) and bile extract porcine (B8631) were purchased from Sigma-Aldrich, St. Louis, MO, USA. Refined soybean oil, sodium caseinate (SC), sodium azide, sodium dihydrogen phosphate, disodium hydrogen phosphate, sodium chloride, methanol (HPLC grade) and dichloromethane (HPLC grade) were procured from Wako Pure Chemical Industries (Osaka, Japan). SC is a large molecular weight emulsifier derived from bovine milk and stabilized the emulsion system by an electrostatic repulsion mechanism. Modified lecithin (ML, SLP White Lyso) was purchased from Tsuji Oil Mills Co. Ltd. (Tokyo, Japan). The ML used in this study is an enzymatically modified phospholipid that was derived from hydrolysis of soy lecithin and composed of a mixture of different phospholipids including phosphatidic acid (0–5%), phosphatidylcholine (2–8%), phosphatidylethanolamine (1–7%), lysophosphatidylcholine (18–30%) and phosphatidylinositol (10–20%). ML and SC were used for evaluating the physicochemical stability of AXT loaded O/W nanoemulsions. Milli-Q water having resistivity of 18 MΩ cm was used for preparing all the solutions and aqueous phase. All other chemicals used in this study were of analytical grade.

2.2. Formulation of astaxanthin-loaded O/W nanoemulsions

The oil phase was prepared by dissolving 4% (w/w) Zanthin® in refined soybean oil (stirring overnight and filtered with 0.45 μm membrane). Filtering was required to remove any insoluble particles that may interfere with nanoemulsion formation or droplet size measurement. The aqueous phase was prepared by dissolving 2.0% (w/w) emulsifier (either SC, or ML) in Milli-Q water containing 0.02% (w/w) NaN_3. The AXT nanoemulsions were formulated using a two-step homogenization method. Firstly, a coarse emulsion was prepared by mixing 10% (w/w) oil phase and 90% (w/w) water phase *via* a rotor-stator homogenizer (Polytron, PT-3000 Kinematica-AG, Littace, Switzerland) at 10,000 rpm for 5 min. In the second step, the fine nanoemulsions were obtained by passing the coarse emulsions through a high-pressure homogenizer (NanoVater, NV200, Yoshida Kikai, Japan) at 100 MPa for 4 passes.

2.3. Physical stability assessment of astaxanthin loaded nanoemulsions

2.3.1. Effect of pH

The nanoemulsions were diluted with the same volume of phosphate buffer (5 mM, pH 7) and the mixture was adjusted to different pH values (2, 4, 6 and 8) using 1 mol L^{-1} HCl or 1 mol L^{-1} NaOH solution. The samples were then transferred to glass vials and stored at room temperature overnight before analysis.

2.3.2. Effect of NaCl

The nanoemulsions (2 mL) were placed in glass vials, and the final salt concentration was adjusted to a range of 0–500 mM by adding 2 mL of NaCl solution. Samples were gently mixed and then stored at room temperature overnight prior to analysis.

2.3.3. Effect of freeze-thaw treatment

The nanoemulsions were transferred to separate plastic test tubes. The test samples were placed at − 20 °C for 22 h, and then left to thaw in a water bath at 30 °C for 2 h prior to droplet size measurement.

2.3.4. Effect of thermal treatment

The nanoemulsion samples were transferred to a glass test tube and sealed using a metallic cap. The samples were placed in water bath or autoclaving machine (KTS-2346, ALP Co., Ltd., Tokyo, Japan) at 60, 90 or 120 °C for 30 min. The mean droplet size and AXT concentration was measured after cooling at room temperature for 90 min.

2.4. Storage stability of astaxanthin loaded nanoemulsions

The nanoemulsions were incubated at 25 °C for 30 days. The mean droplet size and AXT content in the nanoemulsions were measured. The AXT encapsulation efficiency (EE) in samples was calculated according to the following equation:

$$EE\ (\%) = \frac{C_t}{C_0} \times 100 \quad (1)$$

where C_t is the concentration of AXT at a specific time, while C_o is the initial concentration of AXT in the nanoemulsions.

2.5. Droplet size analysis

The measurement of mean droplet size was conducted using a laser diffraction particle size analyzer (LS 13320, Beckman Coulter, Brea, USA) which have tendency to measure the particle size in the range between 0.04 μm and 2000 μm. The refractive indexes of the oil and

water phases used in the measurement were 1.471 and 1.333, respectively. The particle size of the nanoemulsions was expressed as Sauter mean diameter ($d_{3,2}$) or volume mean diameter ($d_{4,3}$). The measurement of each sample was repeated in triplicate.

2.6. ζ-Potential measurement

Determination of the ζ-potential of nanoemulsions droplet was performed by using a ζ-potential analyzer (Zetasizer Nano ZS, Malvern Instruments Ltd., Worcestershire, UK). Before analysis, the nanoemulsions were diluted (1:200) with phosphate buffer (5 mM) with the same pH as samples tested. The ζ-potential of samples were automatically measured using 10–100 runs per analysis after they were equilibrated for 60 s inside the instrument at 25 °C. The refractive indexes of the dispersed and continuous phases for calculation were set at 1.471 and 1.333, respectively. The measurement was conducted in triplicate.

2.7. Quantification of astaxanthin in nanoemulsion system

AXT in nanoemulsion samples was extracted using solvent: 80 μL of nanoemulsion samples were diluted in to 10 mL organic solvent (dichloromethane:methanol = 2:1(v/v)), and then centrifuged at 10,000 rpm for 20 min. AXT was quantified in the supernatant using UV/VIS/NIR spectrophotometer (V-570, JASCO Co., Hachioji, Japan) at 480 nm. The pure methanol and dichloromethane solution as a blank. AXT concentration was calculated from a standard curve (R^2 = 0.9952, n = 5) and expressed in μg mL^{-1}. The measurements were conducted in triplicate.

2.8. In vitro small intestinal digestion

Before digestion, the nanoemulsion was diluted 10 times using phosphate buffer (5 mM, pH 7). Therefore, the samples used to be digested contained 1% oil. An *in vitro* digestion model simulating the small intestine was used to study the influence of emulsion composition on AXT bioaccessibility. The methods of Ahmed, Li, McClements, and Xiao (2012), Calligaris et al. (2015) and Mun, Decker, Park, Weiss, and McClements (2006) were followed with some modifications. 30 g samples were heated at 37 °C for 10 min in a water bath with continuous stirring at 100 rpm min^{-1}. Then, 4 mL bile extract (46.9 g L^{-1} in phosphate buffer at pH 7) and 1 mL calcium chloride (110 g L^{-1} in Milli-Q water) were added. The pH was adjusted to 7. Finally, 2.5 mL of freshly prepared pancreatin suspension (24 g L^{-1} in phosphate buffer at pH 7) was added to the mixture. The pH of the mixture was monitored and maintained at 7 by manually adding 0.5 mol L^{-1} NaOH. The volume of NaOH added to the sample was recorded and used to calculate the percentage of free fatty acids (FFAs) generated during lipolysis. The extent of lipolysis was determined as follows:

$$\text{FFAs}\,(t) = 100 \times \left(\frac{V_{\text{NaOH}}(t) \bullet C_{\text{NaOH}} \bullet M_{\text{oil}}}{2 \bullet m_{\text{oil}}} \right) \quad (2)$$

Here, $V_{\text{NaOH}}(t)$ is the volume of NaOH solution required to neutralize the FFAs produced at digestion time t (L), C_{NaOH} is the molarity of the NaOH solution used to titrate the sample (mol L^{-1}), M_{oil} is the molecular weight of the oil (g/mol), and m_{oil} is the total mass of lipid initially present in the incubation cell (g).

2.9. Separation of micellar fraction and bioaccessibility analysis

The bioaccessibility of AXT was evaluated after the *in vitro* digestion was completed. The digesta was centrifuged at 12,500 rpm for about 60 min. After centrifugation, the sample was separated into an opaque sediment phase (pellet) and a clear phase containing the mixed micelles (supernatant). The collected supernatant was passed through a filter (0.45 μm) and assumed to be the micelles fraction, in which the AXT was solubilized. The AXT micelles fraction was extracted with a solvent extraction method: 1 mL of samples were mixed with 4 mL organic solvent (dichloromethane:methanol = 2:1(v/v)), and then centrifuged at 10,000 rpm for 20 min. The transparent lower organic phase containing the AXT was removed and quantified on spectrophotometer. The bioaccessibility and stability of AXT after digestion were calculated based on the following equation:

$$\text{Bioaccessibility}\,(\%) = \frac{C_{\text{Micelles}}}{C_{\text{Initial}}} \times 100 \quad (3)$$

where C_{Micelles} the concentrations of astaxanthin in micelles fraction, C_{Initial} is the concentration of astaxanthin calculated according to the initial amount added.

2.10. Microstructure analysis

Confocal scanning laser microscopy (Leica TCS SP8, Leica Microsystems Inc., Germany) was used to observe the microstructural changes of nanoemulsion sample before and after passing through digestion stage. Prior to confocal microscopy observation, 1 mL of each nanoemulsion sample was mixed with 0.05 mL of Nile Red solution (1 mg mL^{-1} in ethanol) to locate the lipid phase. An oil-immersion objective lens was used to capture all microstructure images.

2.11. Statistical analysis

All experiments were performed at least three times. One-way analysis of variance (ANOVA) was performed using Statistix 8.1 software (Tallahassee, USA) and least significant difference (LSD) was calculated at the 95% probability level.

3. Results and discussion

3.1. Formulation of nanoemulsions encapsulating astaxanthin

AXT loaded nanoemulsions were formulated by homogenizing 10% (w/w) of oil phase and 90% (w/w) of aqueous phase. Fig. 1a shows the $d_{3,2}$ and $d_{4,3}$ of nanoemulsions stabilized by SC and ML. The $d_{4,3}$ of SC and ML stabilized nanoemulsions were 144 ± 12 nm and 163 ± 5 nm, respectively. Moreover, the freshly prepared nanoemulsions exhibit monomodal droplet size distribution (Fig. 1b) with $d_{3,2}$ ranged between 115 and 136 nm. The freshly prepared nanoemulsions stabilized by either SC or ML retain about 400 μg mL^{-1} of total AXT. The small molecular weight emulsifiers adsorb quickly on the newly created interface and result in small droplet size in comparison to higher molecular weight emulsifiers (Dickinson, 2009; Mao et al., 2009). However, we observed smaller $d_{3,2}$ for SC that constitute large molecular network in comparison to ML. A possible explanation for this variation is the relatively high concentration of SC used in this study. The high concentration provides better coverage at the newly created interface and prevents droplet coalescence (Dickinson, 2009). Most of the nanoemulsions have good stability against droplet growth, but different storage conditions and environmental factors may affect the stability. The effect of different environmental factors on AXT loaded nanoemulsions are described below.

3.2. Effect of pH

Different food products and beverages require different operating pHs. To check the broad functionality of AXT nanoemulsions, the effect of pH was investigated. Fig. 2a presents the change in $d_{4,3}$ of SC and ML stabilized nanoemulsions with varying pH. The $d_{4,3}$ of nanoemulsions stabilized by ML remained constant with varying pH, however, there was phase separation at pH 4 in nanoemulsions stabilized by SC. The nanoemulsion samples are highly unstable with an observable serum layer at the bottom. At other pHs the $d_{4,3}$ remained constant with slight

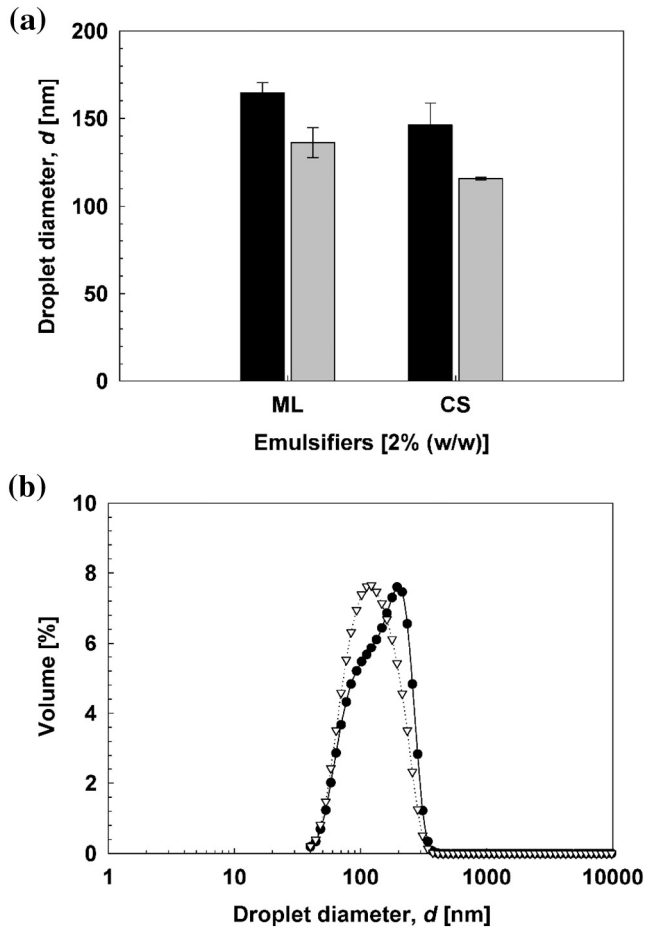

Fig. 1. Effect of modified lecithin (ML) and sodium caseinate (SC) on formulation of O/W nanoemulsions. (a) Sauter mean droplet diameter (■, $d_{4,3}$) and volume mean droplet diameter (▭, $d_{3,2}$) of O/W nanoemulsions. (b) Droplet size distribution of ML and -SC stabilized nanoemulsions. (–●–) denotes ML and (–▽–) denotes SC.

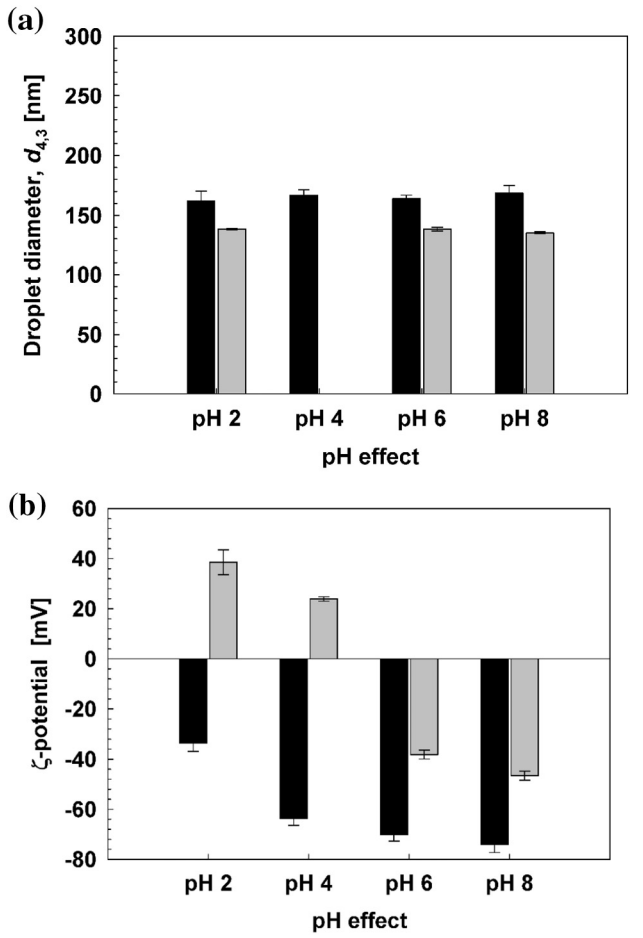

Fig. 2. Effect of pH on the stability of AXT loaded nanoemulsions. (a) $d_{4,3}$ and (b) ζ-potential of AXT loaded nanoemulsions. (■) denotes ML and (▭) denotes SC-stabilized nanoemulsions.

variation.

The effect of pH on the ζ-potential of emulsified samples is presented in Fig. 2b. ζ-Potential absolute value > 30 mV was considered an indicative value that showed stability of droplet aggregation and coalescence (Jourdain, Leser, Schmitt, Michel, & Dickinson, 2008). For SC-stabilized nanoemulsions treated with pH 4, the absolute value of ζ-potential between the droplets was low (< 30 mV), which was attributed to the pH being close to the isoelectric point (≈ pH 4.7). As a result, the electrostatic repulsion was insufficient to prevent the droplets from coming together. In the case of ML-stabilized nanoemulsions, the high stability can be explained by the negative charge on the droplets across the entire pH range, which prevents emulsion droplets from aggregating. SC-stabilized nanoemulsions exhibited a positive charge at pH 2 and 4 since this was below the isoelectric point of 4.7 for the protein (amines are positively charged at this pH), while ML-stabilized emulsions were negatively charged due to the anionic phosphate groups.

3.3. Effect of ionic strength

Emulsified food and beverages often contain different minerals either naturally or through fortification. These minerals can influence the stability and composition of the final products. Therefore, we investigated the influence of ionic strength on the physical stability of AXT loaded nanoemulsions. The addition of NaCl from 0 to 500 mM, resulted in no apparent changes in $d_{4,3}$ of nanoemulsions stabilized by SC (Fig. 3a). The addition of salt to protein-stabilized nanoemulsions resulted in destabilization of emulsions and may be attributed to electrostatic screening effects (H. Kim, Decker, & McClements, 2002; McClements, 2004). The electrostatic screening effect of electrolytes was low for the nanoemulsions stabilized by SC. The electrostatic repulsion between the SC-coated droplets was still strong enough to prevent the droplet coalescence. This effect also was confirmed by the data in Fig. 3b, which shows that there was no distinct change in the magnitude of ζ-potential in the presence of added salt.

In contrast, oiling off was observed on the top of the ML-stabilized nanoemulsions at ≥ 300 mM NaCl and there was increase in $d_{4,3}$ of the samples when NaCl concentration exceeded 300 mM. Similar results have been reported previously (McClements, 2004; Shu et al., 2016). Moreover, NaCl addition might reduce the electrostatic repulsion between the oil droplets at high concentration and promote destabilization in O/W nanoemulsions (Ozturk, Argin, Ozilgen, & McClements, 2014). However, this electrostatic screening effect was not observed, as shown from the ζ-potential values, either for the ML or SC-stabilized nanoemulsions (Fig. 3b). We believe that NaCl addition at high concentration might hydrate the ML molecules polar heads that cause destabilization and creaming in ML-stabilized nanoemulsions (McClements, Decker, & Choi, 2014).

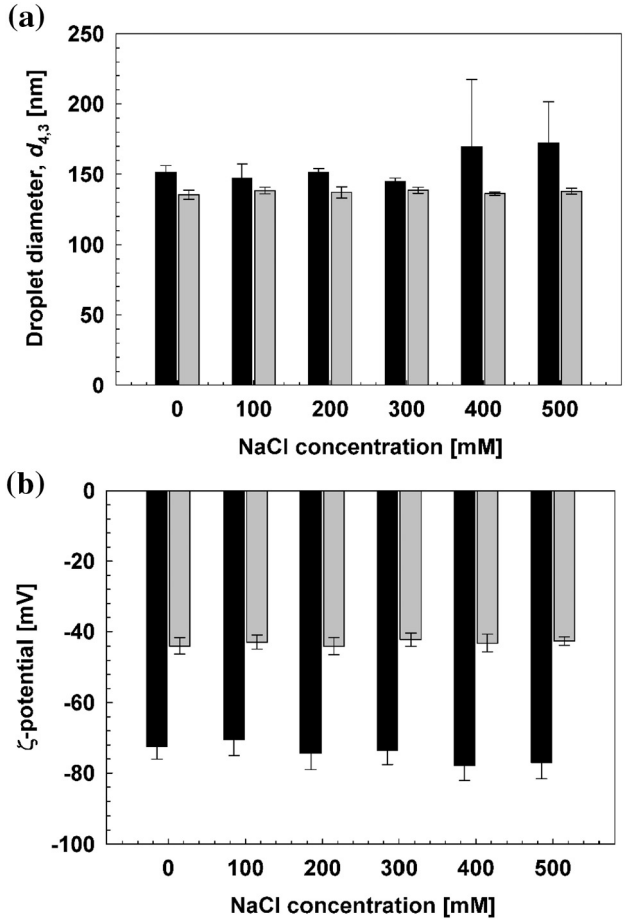

Fig. 3. Effect of NaCl concentration on (a) $d_{4,3}$ and (b) ζ-potential of AXT loaded nanoemulsions. (■) denotes ML and (▭) denotes SC-stabilized nanoemulsions.

3.4. Effect of freeze-thaw treatment

Some emulsified foods are processed at relatively low temperatures, like ice-creams. The stability of these products under freeze-thaw conditions are major challenging in the food industry. Results indicated (Fig. 4) that the ML-stabilized nanoemulsions showed a prominent ($p = 0.02$, < 0.05) increase in $d_{4,3}$ from 136 to 403 nm after four cycles of freeze-thawing. On the other hand, for the SC-stabilized nanoemulsions, the $d_{4,3}$ also significantly increase ($p = 0.01$, < 0.05) from 115 nm to 150 nm after 4 cycles. The results indicated that SC was more resistance to oil droplet coalescence than ML when exposed to freeze-thawing cycles. An increase in droplet size is indicative of emulsion instability since it shows droplet coalescence.

Crystallization is the major problem during freeze-thawing, since water droplets in the emulsified phase come closer together during freezing in between the non-frozen aqueous phase (Ghosh & Coupland, 2008). Emulsifier plays a prominent role in reducing the contraction of water droplets and the aggregation process. Protein based emulsifiers formed a thick layer around the interface and inhibit droplet aggregation and coalescence. The high concentration of SC restricts the movement of water molecule to a small extent and reduces the variation of $d_{4,3}$ in AXT loaded nanoemulsions in comparison to ML-coated nanoemulsions.

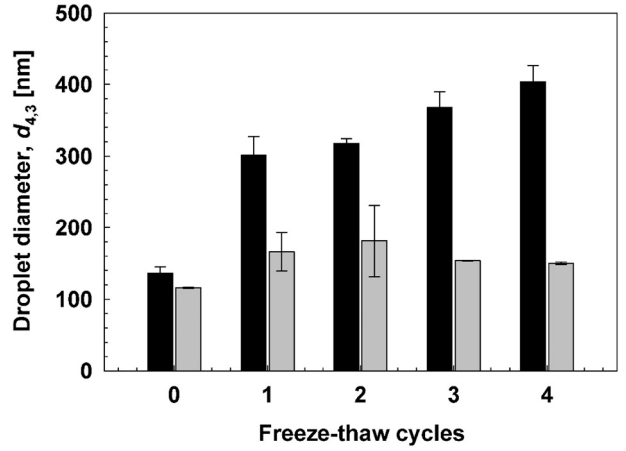

Fig. 4. Effect of freeze-thawing on the stability of AXT loaded nanoemulsions. The change in $d_{4,3}$ of nanoemulsions. (■) denotes ML and (▭) denotes SC-stabilized nanoemulsions.

3.5. Effect of high temperature treatment

We evaluated the effect of high temperature (60, 90 and 120 °C) on the stability of AXT-loaded nanoemulsions. High temperature is often used during food processing, such as during pasteurization, hot filling and autoclaving. An appreciable increase in $d_{4,3}$ was observed at 120 °C in nanoemulsions stabilized by SC (Fig. 5a), that strongly correlated with increased droplet aggregation over time. However, no oil droplet growth was observed in ML-stabilized nanoemulsions at elevated temperatures. There was non-significant difference (Fig. 5b, $p = 0.08$, > 0.05) among retention profiles of AXT in SC or ML-stabilized nanoemulsions. The decrease in retention of AXT varied from 14 to 18% in SC or ML-stabilized nanoemulsions.

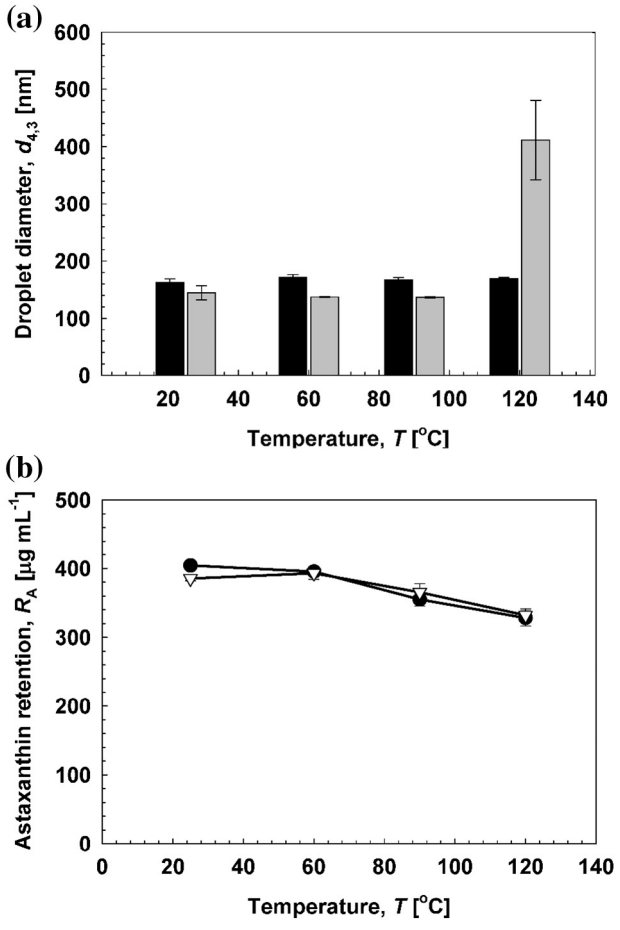

Fig. 5. Effect of heating temperature on $d_{4,3}$ and chemical stability of AXT loaded nanoemulsions. (a) Effect of heating temperature. (■) denotes ML and (▭) denotes SC-stabilized nanoemulsions. (b) Chemical stability of nanoemulsions after heat treatment. (–●–) denotes ML and (–▽–) denotes SC-stabilized nanoemulsions.

SC is quite stable at high temperature due to its disordered structure (Srinivasan, Singh, & Munro, 2002), but the aggregation of droplets in our study might be due to dephosphorization of caseinate molecules at high temperature that promotes caseinate-caseinate interactions and weaken the interfacial layers around the oil droplets (Chu, Ichikawa, Kanafusa, & Nakajima, 2008; O'Regan & Mulvihill, 2010). The droplets growth was not observed in ML-stabilized nanoemulsions, which suggested that the electrostatic repulsion between ML-coated droplets was strong enough to overcome the attractive interactions and prevent droplets aggregation at elevated temperatures.

3.6. Long-term storage stability

Long-term stability of AXT loaded nanoemulsions was investigated at 25 °C for a period of 30 days using ML and SC as emulsifiers. Fig. 6 showed variation in $d_{4,3}$ of AXT loaded nanoemulsions during 30 days of storage. The stored nanoemulsions showed good stability against phase creaming, phase separation and oil droplet growth. The $d_{4,3}$ remained between 166 and 169 nm ($p = 0.12$, > 0.05) in ML-stabilized nanoemulsions and between 137 and 139 ($p = 0.13$, > 0.05) in SC-stabilized nanoemulsions (Fig. 6a). The small sized oil droplets in the emulsion system resist gravitational separation and coalescence (McClements, 2012). Moreover, due to long chain triglycerides (soybean oil) structure, the Oswald ripening is limited, further stabilizing the nanoemulsions (Wooster, Golding, & Sanguansri, 2008).

The long-term AXT stability of nanoemulsions stored at 25 °C was evaluated by determining the change in retention of AXT during 30 days of storage. The fresh O/W nanoemulsions stabilized by ML and SC contained 400 ± 5.0 and 385.2 ± 3.3 μg mL^{-1} AXT, respectively. The retentions of AXT at day 0 is regarded as 100% (Fig. 6b). There was sharp decline in retention of AXT in ML-stabilized nanoemulsions to 178 μg mL^{-1} after 30 days of storage. A similar trend was observed in SC-stabilized nanoemulsions and with a decrease in AXT concentration from 385 to 283 μg mL^{-1} after 30 days of storage. The long-term AXT stability of nanoemulsions indicated that SC was more effective at preventing AXT from degradation, which was associated with its iron-chelating and anti-oxidative properties, and also the capability of forming a thick protective layer around the oil droplets (Hu, McClements, & Decker, 2003).

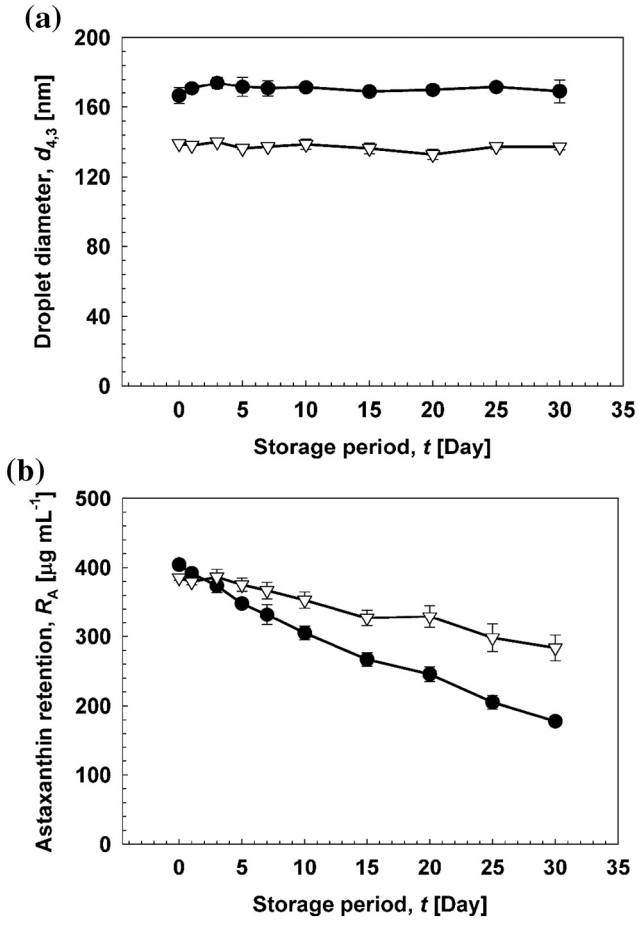

Fig. 6. Effect of storage temperature on physical and chemical stability of AXT loaded nanoemulsions. (a) physical stability of O/W nanoemulsions. (b) chemical stability of AXT loaded nanoemulsions at 25 °C. (–●–) denotes ML and (–▽–) denote SC-stabilized nanoemulsions.

3.7. Effect of emulsifiers on astaxanthin bioaccessibility

The influence of ML and SC on the bioaccessibility of AXT was evaluated by measuring the AXT concentrations in the micelle fraction. Moreover, the kinetics of AXT digestion was monitored by measuring FFA release over time, when nanoemulsions were mixed with simulated digestion fluids. The initial rate of FFA release (Fig. 7a) was faster in ML-stabilized nanoemulsions than in SC-stabilized nanoemulsions,

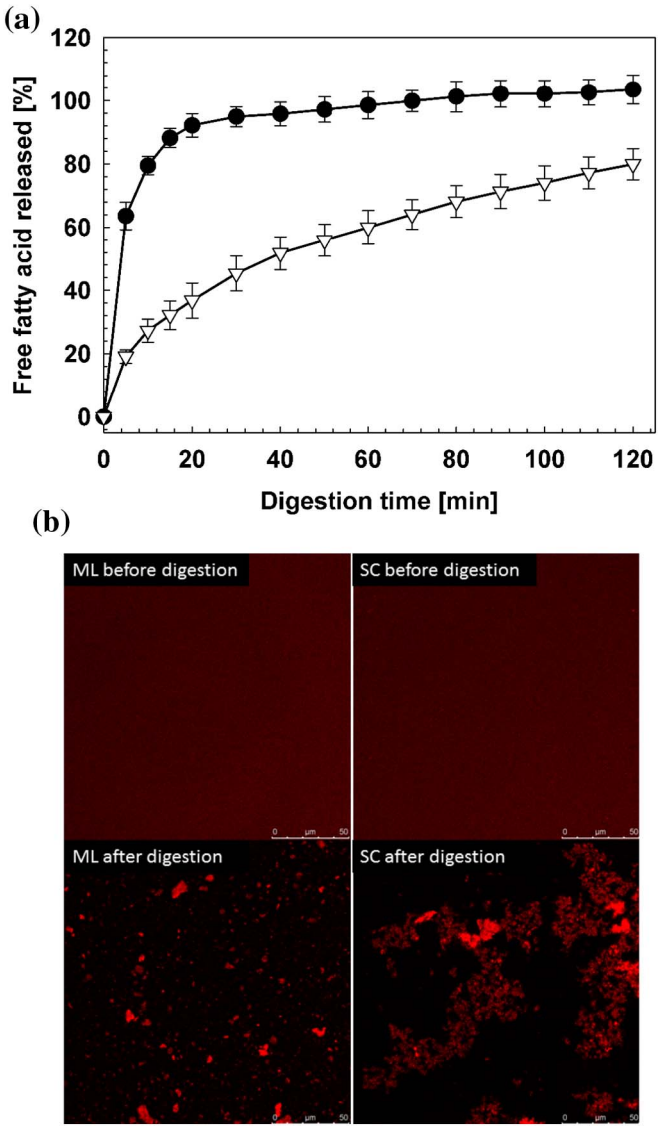

Fig. 7. *In vitro* digestion studies of ML and SC-stabilized O/W nanoemulsions. (a) Influence of ML and SC on the release of FFAs from nanoemulsions loaded with AXT during digestion. (–●–) denotes ML and (–▽–) denote SC-stabilized nanoemulsions. (b) Microstructure (confocal microscopy) of AXT loaded nanoemulsions before and after exposure to *in vitro* digestion model.

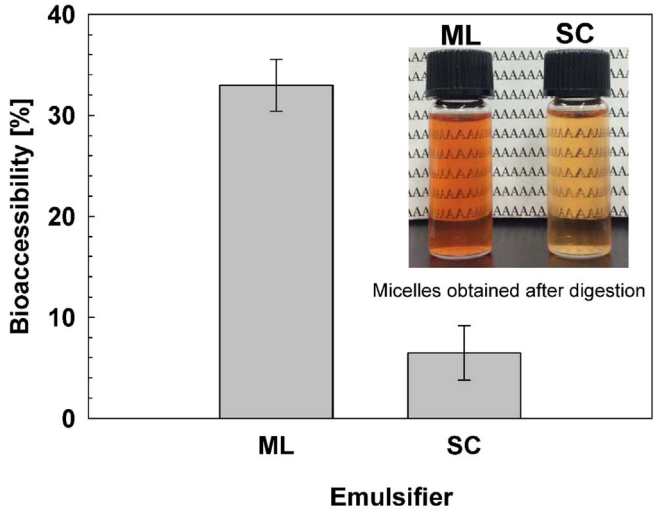

Fig. 8. Influence of ML and SC on the bioaccessibility of AXT in nanoemulsion-based delivery system.

during the first 10 min of digestion, and this was followed by a more gradual increase after 110 min of digestion. The observed slow FFA release rate in SC-stabilized nanoemulsions might be because the calcium bridging in SC caused aggregation of oil droplets, thereby reducing exposed surface area in the emulsion system. The small surface area restricted the pancreatin from penetrating into the droplets. Moreover, due to calcium bridging there might be reduction of calcium ions in simulated digestion fluid (Dickinson & Golding, 1998). The calcium ions play a vital role in lipid digestion. The other possible reason for slow releasing of FFA is the thick interfacial layer around the oil droplets that inhibits pancreatin attack.

Even with higher production of FFA, the bioaccessibility of AXT in ML-stabilized nanoemulsions was > 32%. The confocal laser micrographs also showed less oil droplet aggregates (Fig. 7b), which indicates higher bioaccessibility of AXT. On the other hand, the bioaccessibility of AXT in SC-stabilized nanoemulsions was only 6% (Fig. 8), which was much lower than the ML-stabilized nanoemulsions, with oil droplet aggregates visualized in the micrograph of SC-stabilized nanoemulsions after digestion. Several potential reasons could account for this phenomenon: (i) The inhibition of FFAs released from SC-stabilized nanoemulsions resulted in less formation of mixed micelles; (ii) the oil fraction was not fully digested for the SC based nanoemulsions, thus, more AXT was retained with this undigested oil; or (iii) the interaction between AXT with casinate molecules may promote the aggregation and precipitation of mixed micelles during digestion.

4. Conclusion

The study showed successful formulation of AXT-loaded nanoemulsions *via* a high-pressure homogenization method. Both ML and SC as emulsifiers effectively stabilized the O/W nanoemulsions. However, the physicochemical stability of AXT nanoemulsions was strongly dependent on various environmental stresses and the nature of the emulsifiers. Selection of emulsifier depends upon pH, temperature and freeze-thawing requirements. “The chemical stability was higher for SC-stabilized nanoemulsions than for ML-stabilized nanoemulsions. However, much higher bioaccessibility of AXT was observed in ML-stabilized nanoemulsions, mainly due to greater formation of mixed micelles. The optimized ML-stabilized nanoemulsion system is probably the better system for use in new functional beverage products, since it has both a good release profile and reasonable stability.” The results of our study provide information useful for selecting appropriate emulsifier for producing AXT loaded aqueous products and also new functional products that contain high concentrations of AXT.

References

Affandi, M., Julianto, T., & Majeed, A. (2011). Development and stability evaluation of astaxanthin nanoemulsion. *Asian Journal of Pharmaceutical and Clinical Research*, *4*(1), 142–148.

Ahmed, K., Li, Y., McClements, D. J., & Xiao, H. (2012). Nanoemulsion-and emulsion-based delivery systems for curcumin: Encapsulation and release properties. *Food Chemistry*, *132*(2), 799–807.

Anarjan, N., Jafarizadeh Malmiri, H., Ling, T. C., & Tan, C. P. (2014). Effects of pH, ions, and thermal treatments on physical stability of astaxanthin nanodispersions. *International Journal of Food Properties*, *17*(4), 937–947.

Anarjan, N., Mirhosseini, H., Baharin, B. S., & Tan, C. P. (2010). Effect of processing conditions on physicochemical properties of astaxanthin nanodispersions. *Food Chemistry*, *123*(2), 477–483.

Anarjan, N., & Tan, C. P. (2013a). Chemical stability of astaxanthin nanodispersions in orange juice and skimmed milk as model food systems. *Food Chemistry*, *139*(1), 527–531.

Anarjan, N., & Tan, C. P. (2013b). Developing a three component stabilizer system for producing astaxanthin nanodispersions. *Food Hydrocolloids*, *30*(1), 437–447.

Calligaris, S., Comuzzo, P., Bot, F., Lippe, G., Zironi, R., Anese, M., & Nicoli, M. C. (2015). Nanoemulsions as delivery systems of hydrophobic silybin from silymarin extract: Effect of oil type on silybin solubility, in vitro bioaccessibility and stability. *LWT - Food Science and Technology*, *63*(1), 77–84.

Chen, J.-T., & Kotani, K. (2016). Astaxanthin as a potential protector of liver function: A review. *Journal of Clinical Medicine Research*, *8*(10), 701.

Chen, Y.-T., Kao, C.-J., Huang, H.-Y., Huang, S.-Y., Chen, C.-Y., Lin, Y.-S., ... Wang, H.-M. D. (2017). Astaxanthin reduces MMP expressions, suppresses cancer cell migrations, and triggers apoptotic caspases of in vitro and in vivo models in melanoma. *Journal of Functional Foods*, *31*, 20–31.

Chu, B. S., Ichikawa, S., Kanafusa, S., & Nakajima, M. (2008). Stability of protein-stabilised β-carotene nanodispersions against heating, salts and pH. *Journal of the Science of Food and Agriculture*, *88*(10), 1764–1769.

Dickinson, E. (2009). Hydrocolloids as emulsifiers and emulsion stabilizers. *Food Hydrocolloids*, *23*(6), 1473–1482.

Dickinson, E., & Golding, M. (1998). Influence of calcium ions on creaming and rheology of emulsions containing sodium caseinate. *Colloids and Surfaces A: Physicochemical and Engineering Aspects*, *144*(1), 167–177.

Dose, J., Matsugo, S., Yokokawa, H., Koshida, Y., Okazaki, S., Seidel, U., ... Esatbeyoglu, T. (2016). Free radical scavenging and cellular antioxidant properties of astaxanthin. *International Journal of Molecular Sciences*, *17*(1), 103.

Foss, B. J., Sliwka, H.-R., Partali, V., Naess, S. N., Elgsaeter, A., Melø, T. B., ... Lockwood, S. F. (2005). Hydrophilic carotenoids: Surface properties and aqueous aggregation of a rigid, long-chain, highly unsaturated dianionic bolaamphiphile with a carotenoid spacer. *Chemistry and Physics of Lipids*, *135*(2), 157–167.

Ghosh, S., & Coupland, J. N. (2008). Factors affecting the freeze–thaw stability of emulsions. *Food Hydrocolloids*, *22*(1), 105–111.

Gutiérrez, J., González, C., Maestro, A., Sole, I., Pey, C., & Nolla, J. (2008). Nano-emulsions: New applications and optimization of their preparation. *Current Opinion in Colloid & Interface Science*, *13*(4), 245–251.

Hu, M., McClements, D. J., & Decker, E. A. (2003). Lipid oxidation in corn oil-in-water emulsions stabilized by casein, whey protein isolate, and soy protein isolate. *Journal of Agricultural and Food Chemistry*, *51*(6), 1696–1700.

Ishikawa, S., Hashizume, K., Nishigori, H., Tezuka, Y., Sanbe, A., & Kurosaka, D. (2015). Effect of astaxanthin on cataract formation induced by glucocorticoids in the chick embryo. *Current Eye Research*, *40*(5), 535–540.

Jourdain, L., Leser, M. E., Schmitt, C., Michel, M., & Dickinson, E. (2008). Stability of emulsions containing sodium caseinate and dextran sulfate: Relationship to complexation in solution. *Food Hydrocolloids*, *22*(4), 647–659.

Kim, D. M., Hyun, S. S., Yun, P., Lee, C. H., & Byun, S. Y. (2012). Identification of an emulsifier and conditions for preparing stable nanoemulsions containing the antioxidant astaxanthin. *International Journal of Cosmetic Science*, *34*(1), 64–73.

Kim, H., Decker, E., & McClements, D. (2002). Impact of protein surface denaturation on droplet flocculation in hexadecane oil-in-water emulsions stabilized by β-lactoglobulin. *Journal of Agricultural and Food Chemistry*, *50*(24), 7131–7137.

Kittikaiwan, P., Powthongsook, S., Pavasant, P., & Shotipruk, A. (2007). Encapsulation of *Haematococcus pluvialis* using chitosan for astaxanthin stability enhancement. *Carbohydrate Polymers*, *70*(4), 378–385.

Lerfall, J., Bendiksen, E.Å., Olsen, J. V., Morrice, D., & Østerlie, M. (2016). A comparative study of organic-versus conventional farmed Atlantic salmon. I. Pigment and lipid content and composition, and carotenoid stability in ice-stored fillets. *Aquaculture*, *451*, 170–177.

Liu, X., McClements, D. J., Cao, Y., & Xiao, H. (2016). Chemical and physical stability of astaxanthin-enriched emulsion-based delivery systems. *Food Biophysics*, *11*(3), 302–310.

Mao, L., Xu, D., Yang, J., Yuan, F., Gao, Y., & Zhao, J. (2009). Effects of small and large molecule emulsifiers on the characteristics of b-carotene nanoemulsions prepared by high pressure homogenization. *Food Technology and Biotechnology*, *47*(3), 336–342.

Mason, T., Wilking, J., Meleson, K., Chang, C., & Graves, S. (2006). Nanoemulsions: Formation, structure, and physical properties. *Journal of Physics: Condensed Matter*, *18*(41), R635.

McClements, D. J. (2004). Protein-stabilized emulsions. *Current Opinion in Colloid & Interface Science*, *9*(5), 305–313.

McClements, D. J. (2012). Nanoemulsions versus microemulsions: Terminology, differences, and similarities. *Soft Matter*, *8*(6), 1719–1729.

McClements, D. J., Decker, E. A., & Choi, S. J. (2014). Impact of environmental stresses on

orange oil-in-water emulsions stabilized by sucrose monopalmitate and lysolecithin. *Journal of Agricultural and Food Chemistry*, *62*(14), 3257–3261.

McClements, D. J., & Rao, J. (2011). Food-grade nanoemulsions: Formulation, fabrication, properties, performance, biological fate, and potential toxicity. *Critical Reviews in Food Science and Nutrition*, *51*(4), 285–330.

Mun, S., Decker, E. A., Park, Y., Weiss, J., & McClements, D. J. (2006). Influence of interfacial composition on in vitro digestibility of emulsified lipids: Potential mechanism for chitosan's ability to inhibit fat digestion. *Food Biophysics*, *1*(1), 21–29.

O'Regan, J., & Mulvihill, D. M. (2010). Heat stability and freeze–thaw stability of oil-in-water emulsions stabilised by sodium caseinate–maltodextrin conjugates. *Food Chemistry*, *119*(1), 182–190.

Ozturk, B., Argin, S., Ozilgen, M., & McClements, D. J. (2014). Formation and stabilization of nanoemulsion-based vitamin E delivery systems using natural surfactants: Quillaja saponin and lecithin. *Journal of Food Engineering*, *142*, 57–63.

Ozturk, B., & McClements, D. J. (2016). Progress in natural emulsifiers for utilization in food emulsions. *Current Opinion in Food Science*, *7*, 1–6.

Raikos, V., & Ranawana, V. (2017). Designing emulsion droplets of foods and beverages to enhance delivery of lipophilic bioactive components–a review of recent advances. *International Journal of Food Science and Technology*, *52*(1), 68–80.

Ribeiro, H. S., Rico, L. G., Badolato, G. G., & Schubert, H. (2005). Production of O/W emulsions containing astaxanthin by repeated premix membrane emulsification. *Journal of Food Science*, *70*(2), E117–E123.

Salvia-Trujillo, L., Soliva-Fortuny, R. C., Rojas-Graü, M. A., Martín-Belloso, O., & McClements, D. J. (2017). Edible Nanoemulsions as carriers of active ingredients: A review. *Annual Review of Food Science and Technology*, *8*(1).

Shahidi, F., & Ambigaipalan, P. (2015). Novel functional food ingredients from marine sources. *Current Opinion in Food Science*, *2*, 123–129.

Shu, G., Khalid, N., Zhao, Y., Neves, M. A., Kobayashi, I., & Nakajima, M. (2016). Formulation and stability assessment of ergocalciferol loaded oil-in-water nanoemulsions: Insights of emulsifiers effect on stabilization mechanism. *Food Research International*, *90*, 320–327.

Srinivasan, M., Singh, H., & Munro, P. (2002). Formation and stability of sodium caseinate emulsions: Influence of retorting (121 C for 15 min) before or after emulsification. *Food Hydrocolloids*, *16*(2), 153–160.

Surh, J., Decker, E. A., & McClements, D. J. (2006). Influence of pH and pectin type on properties and stability of sodium-caseinate stabilized oil-in-water emulsions. *Food Hydrocolloids*, *20*(5), 607–618.

Tachaprutinun, A., Udomsup, T., Luadthong, C., & Wanichwecharungruang, S. (2009). Preventing the thermal degradation of astaxanthin through nanoencapsulation. *International Journal of Pharmaceutics*, *374*(1), 119–124.

Taksima, T., Limpawattana, M., & Klaypradit, W. (2015). Astaxanthin encapsulated in beads using ultrasonic atomizer and application in yogurt as evaluated by consumer sensory profile. *LWT- Food Science and Technology*, *62*(1), 431–437.

Wooster, T. J., Golding, M., & Sanguansri, P. (2008). Impact of oil type on nanoemulsion formation and Ostwald ripening stability. *Langmuir*, *24*(22), 12758–12765.

Xu, L., Zhu, J., Yin, W., & Ding, X. (2015). Astaxanthin improves cognitive deficits from oxidative stress, nitric oxide synthase and inflammation through upregulation of PI3K/Akt in diabetes rat. *International Journal of Clinical and Experimental Pathology*, *8*(6), 6083.

Zhang, J., Wang, Q.-z., Zhao, S.-h., Ji, X., Qiu, J., Wang, J., & Gao, H. Q. (2017). Astaxanthin attenuated pressure overload-induced cardiac dysfunction and myocardial fibrosis: Partially by activating SIRT1. *Biochimica et Biophysica Acta*. In Press http://dx.doi.org/10.1016/j.bbagen.2017.03.007.